

DWT-OFDM Diversity for TSV-Model Based 60 GHz WPAN System

C N Deshmukh¹, V T Ingole²

Assoc. Prof, Dept of Electronics & Telecommunication Engg., PRMIT&R, Badnera, Maharashtra, India¹

Director, IBSS College of Engineering, Ghatkheda, Amravati, Maharashtra, India²

Abstract: In the context of WLAN (Wireless Local Area Network) and WPAN (Wireless Personal Area Network) systems for High Data Rate (HDR) wireless communications, the unlicensed frequency band available in the millimeter wave region has become more and more attractive. Currently focus is on use of OFDM system to cater for increased data rate of wireless medium with good performance. Diversity techniques play an important role in achieving higher performance level for limited power wireless systems. Wavelet analysis has some strong advantages over Fourier analysis, as it allows a time-frequency domain operation, allowing optimal resolution and flexibility. Wavelets have been satisfactorily used in almost all the fields of wireless communication systems including OFDM which is a strong candidate for next generation of wireless system. This paper proposes a DWT-OFDM Diversity to achieve better performance in terms of SNR and bit error rate (BER) for TSV model based channel at 60 GHz. The performances of different discrete wavelets for channels defined by IEEE 802.15.4a are analyzed. The results indicate better BER performance in case of lower order wavelet.

Keywords: DWT, OFDM, TSV Model, WPAN, WLAN, FFT, SNR, BER, ISI

I. INTRODUCTION

During the past few years, substantial knowledge about the 60-GHz millimeter-wave (MMW) channel has been accumulated and a great deal of work has been done toward developing MMW communication systems for commercial applications. In 2001, the Federal Communications Commission (FCC) allocated 7 GHz in the 57–64 GHz band for unlicensed use. The opening of that big chunk of free spectrum, combined with advances in wireless communications technologies, has rekindled interest in this portion of spectrum once perceived for expensive point-to-point (P2P) links. The immediately seen opportunities in this particular region of spectrum include next-generation wireless personal area networks (WPANs).

The abundance of the bandwidth in the unlicensed 60 GHz band is unmatched in any of the lower frequency bands. The fact that this band is unlicensed and largely harmonized across most regulatory regions in the world is a big advantage, in contrast with the meager spectrum available in the lower frequency bands for existing technologies such as Wi-Fi. The 60 GHz band boasts a wide spectrum of up to 9 GHz that is typically divided into channels of roughly 2 GHz each. Such wide channels make it easy to achieve gigabit data rate even with relatively simple modulation and coding schemes.

OFDM technique promises better performance for this WPAN system due to certain diversity advantage. In Orthogonal Frequency Division Multiplexing (OFDM) the signal itself is first split into independent channel, modulated by data and further re-multiplexed to create OFDM carrier. As the subcarriers in OFDM are orthogonal, it allows simultaneous transmission of multiple sub carriers in a compact frequency space without interference. OFDM can provide large data rates even under channel impairment. Efficient compact spectral

utilization can be achieved in OFDM scheme with help of minimally separated sub-carriers [5]. Similarly OFDM scheme convert a broadband frequency selective channel into parallel flat fading narrow band sub channel.

In order to mitigate the problem of ISI (Inter symbol interference) caused by complex multipath wireless channel a cyclic prefix (CP) [4] is added to each symbol in OFDM system. On the other hand wavelet based modulation satisfies orthogonality criterion. We can derive benefits of OFDM even when traditional sinusoid carriers of FFT based OFDM are replaced with suitable wavelets. Wavelet based system have better immunity to impulse and narrow band noises as compared to FFT OFDM[2,4].

In addition to this wavelet based OFDM does not require any CP leading to increase in spectral efficiency, reduce complexity and better symbol rate. Discrete wavelet transform (DWT) are being considered as alternative platforms for replacing IFFT and FFT [15,16]. It utilizes low pass filter and high pass filter operating as Quadrature Mirror Filters (QMF) satisfying perfect reconstruction and orthonormal properties. The purpose of this paper is to demonstrate the diversity advantage provided by use of DWT in place of FFT in OFDM system for wireless personal area network (WPAN).

Section II presents the traditional FFT OFDM and wavelet OFDM whereas **Section III** describes the system and channel model. In **section IV** simulation environment with result are discussed. **Section V** concludes the paper.

II. FFT OFDM AND WAVELET OFDM

A. FFT-OFDM

OFDM system is used as modulation method that divides a given bandwidth into multiple smaller sub-bands. In time domain, an N-point FFT OFDM system can be represented as:

$$s[n] = \frac{1}{\sqrt{N}} \sum_{k=0}^{N-1} S_k e^{j2\pi nk/N}, n=0,1,2,\dots,N-1 \quad (1)$$

Where $s[n]$ is the discrete form of $s(t)$, N is the number of sub-channels, $\frac{1}{\sqrt{N}}$ is a scaling factor with n as the index of the prevalent subcarrier. S_k is the BPSK mapped input symbol of k^{th} sub-channel. The number of FFT points used is same as the number of narrowband sub-channels over which the input symbols are multiplexed. Each of the resulting narrowband sub-channels is modulated by the mapped input bits. Cyclic prefix (CP) at least equal to the length of the channel response, L is pre-appended to each OFDM symbol to contest ISI. To account for the CP, Equation 1 can be expressed as:

$$s[n] = \frac{1}{\sqrt{N}} \sum_{k=0}^{N-1} S_k e^{j2\pi nk/N}, -N_g \leq n \leq N-1 \quad (2)$$

In Equation 2, N_g denotes the length of CP pre-appended to every OFDM symbol.

B. Wavelet – OFDM

The discrete wavelet transform (DWT) can be used to study multicarrier systems as in [9]. It represents signals in time-frequency domain such that the signal exists neither purely in frequency domain nor purely in time domain. For a mapped input symbol S_k to be transformed by the DWT, the time domain output can be realized from [10];

$$s[n] = \sum_k \sum_{m=0}^{M-1} S_{k,n} \varphi_{m,n}(t) \quad (3)$$

where $S_{k,n}$ represents the n^{th} symbol which modulates the m^{th} -waveform of the k^{th} -constellation. $\varphi_{m,n}(t)$ represents the complex orthogonal DWT basis function similar to the traditional OFDM as:

$$\varphi_{m,n} = \begin{cases} 1 & n = m \\ 0 & \text{elsewhere} \end{cases} \quad (4)$$

where m and n are scales and shifts respectively. If n is the index of each discrete wavelet symbol $s[n]$ of the continuous time symbol $s(t)$, then the wavelet transform is defined as [11]:

$$\Psi_{k,a}(t) = e^{j\pi t^2} \quad (5)$$

Now, let a continuous wavelet function is expressed as:

$$\Psi_{k,a}(t) = \frac{1}{\sqrt{k}} \Psi\left(\frac{t-a}{k}\right) \quad (6)$$

where k and a are the scaling and shifting parameters respectively and $\Psi(\cdot)$ is called the mother wavelet. Then, from Equations 5 and 6 the resulting continuous transform can be represented as:

$$S_{CWT}(\tau, k) = \frac{1}{\sqrt{k}} \int_{-\infty}^{\infty} \exp\left[j\pi \frac{(t-\tau)^2}{k^2}\right] s(t) dt \quad (7)$$

Equation 7 has the advantage of time and frequency diversities unlike the FFT transform that has only frequency diversity advantage. In fact, it has been explored that orthogonal wavelet-based OFDM is more robust to ICI and ISI problems than the FFT-based OFDM

[12-14]. Absence of CP in wavelet OFDM unlike that in FFT OFDM, provides for additional 25% spectral efficiency.

III. SYSTEM AND CHANNEL MODEL

A. FFT OFDM MODEL

The OFDM system model described below is utilized for both FFT-OFDM and DWT-OFDM. The input binary data is generated randomly as bit stream b . It is processed using BPSK modulator to map the input data into symbols X_m . These symbols are now passed through IFFT block to perform IFFT operation to generate N parallel data streams. Its output in discrete time domain is given by,

$$X_{k(n)} = \frac{1}{\sqrt{N}} \sum_{i=0}^{N-1} X_m(i) e^{j\frac{2\pi ni}{N}} \quad (8)$$

The cyclic prefix is now appended to transformed output (X_k). The cyclic prefix (CP) is added before transmission, to moderate ISI effect. This OFDM symbol is passed through standard UWB channel. At the receiver, the reverse operation is carried out to obtain the original data back. The CP is removed and processed in the FFT block and finally passed through demodulator for data recovery. The output of the FFT in frequency domain is given by,

$$Y_{m(i)} = \sum_{n=0}^{N-1} Y_{k(n)} e^{-j\frac{2\pi ni}{N}} \quad (9)$$

B. DWT OFDM MODEL

In DWT OFDM, at the transmitter the input data b maps on to BPSK modulator, thereby converting data b_k into symbols $X_{m(i)}$. Each $X_{m(i)}$ is first converted to serial representation having a vector XX which will next be transposed into CA. Then, the signal is up-sampled (zero padding) and filtered by the LPF coefficients or approximated coefficients. Since our aim is to have low frequency signals, the modulated signals XX perform circular convolution with LPF filter whereas the HPF filter also perform the convolution with zeroes padding signals CD respectively. Note that the HPF filter contains detailed coefficients or wavelet coefficients. This data is given as an input to IDWT block wherein a particular wavelet is chosen for simulation. At the receiver, DWT and PSK demodulator (BPSK) are used to recover back the data.

C. Channel Model

The Complex impulse response is given as [17]

$$h(t) = \beta \delta(t) + \sum_{l=0}^{L-1} \sum_{m=0}^{M_l-1} \alpha_{l,m} \delta(t - T_l - \tau_{l,m}) \delta(\phi - \Psi_l - \psi_{l,m})$$

$$|\alpha_{l,m}|^2 = \Omega_0 e^{-T_l/\Gamma} e^{-\tau_{l,m}/\gamma - k[1-\delta(m)]} \sqrt{G_r(0, \Psi_l + \psi_{l,m})}$$

$$\angle \alpha_{l,m} \propto \text{Uniform}[0, 2\pi]$$

PL_d : Path loss of the first impulse response;

t : time[ns]; $d(\cdot)$: Delta function

l = cluster number,

m = ray number in l -th cluster,

L = total number of clusters;

M_l = total number of rays in the l -th cluster;
 T_l = arrival time of the first ray of the l -th cluster;
 $\tau_{l,m}$ = delay of the m -th ray within the l -th cluster relative to the first path arrival time, T_l ;
 W_0 = Average power of the first ray of the first cluster
 $Y_l \propto \text{Uniform}[0, 2\pi)$; arrival angle of the first ray within the l^{th} cluster
 $y_{l,m}$ = arrival angle of the m -th ray within the l^{th} cluster relative to the first path arrival angle, Y_l
 The Two-path response is given as

$$\beta \text{ [dB]} = 20 \cdot \log_{10} \left[\left(\frac{\mu_d}{d} \right) \sqrt{G_{r1}G_{r1} + \sqrt{G_{r2}G_{r2}} \Gamma_0} \exp \left[j \frac{2\pi}{\lambda_f} \frac{2h_1h_2}{d} \right] \right] - PL_d(\mu_d)$$

$$PL_d(\mu_d) \text{ [dB]} = PL_d(d_0) + 10 \cdot n_d \cdot \log_{10} \left(\frac{d}{d_0} \right)$$

$$PL_d(d_0) \text{ [dB]} = 20 \log_{10} \left(\frac{4\pi d_0}{\lambda_f} \right) + A_{NLOS}$$

A_{NLOS} : Constant attenuation for NLOS
 Path number of G_{ri} and G_{ri} (1 : direct, 2 : reflect)

$d \propto \text{Uniform}$: Distance between Tx and Rx,
 $h_1 \propto \text{Uniform}$: Height of Tx
 $h_2 \propto \text{Uniform}$: Height of Rx ,
 $\mu_d \propto \text{Average}$ of distance between Tx and Rx
 $|\Gamma_0|$: Reflection coefficient
 $|\Gamma_0| \cong 1$: LOS Desktop environment (incident angle $\cong \pi/2$)
 $|\Gamma_0| \cong 0$: Other LOS/NLOS environment

Arrival rate: It is described as a Poisson process and given as

$$p(T_l | T_{l-1}) = \Lambda \exp[-\Lambda(T_l - T_{l-1})] \quad l > 0$$

$$p(\tau_l | \tau_{l,(m-1)}) = \lambda \exp[-\lambda(\tau_l - \tau_{l,(m-1)})] \quad m > 0$$

Where

Γ : cluster decay factor
 $1/\Lambda$: cluster arrival rate
 γ : ray decay factor
 $1/\lambda$: ray arrival rate
 σ_1 : cluster lognormal standard deviation
 σ_2 : ray lognormal standard deviation
 σ_ϕ : Angle spread of ray within cluster (Laplace distribution)

Antenna parameters

$$G(\theta, \phi) = G \exp[-\alpha(\theta^2 + \phi^2)]$$

$G_t(\theta, \phi)$: Antennagain of Tx

$G_r(\theta, \iota)$: Antennagain of Rx

Rician factor k: Ray Rician effect is given as

$$K = \frac{\beta^2}{\sum_{l=0}^{L-1} \sum_{m=0}^{M_l-1} \alpha_{l,m}^2 \left| \delta(t - T_l - \tau_{l,m}) \delta(\phi - \Psi_l - \psi_{l,m}) G_r(0, \Psi_l + \psi_{l,m}) \right|^2}$$

IV. SIMULATION ENVIRONMENT WITH RESULT

Channel Model	Environment
CM1	Residential LOS TSV & SV
CM2	Residential NLOS TSV & SV
CM3	Office LOS TSV
CM4	Office NLOS TSV
CM7	Desktop LOS TSV & SV
CM8	Desktop NLOS SV

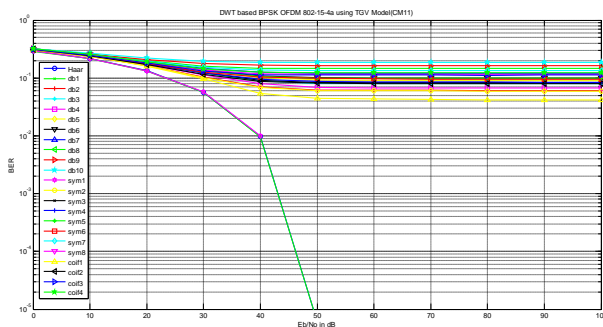
Param.	CM1.1	CM1.2	CM1.3	CM1.4
Λ [1/ns]	0.191	0.194	0.144	0.045
λ [1/ns]	1.22	0.90	1.17	0.93
Γ [ns]	4.46	8.98	21.5	12.6
γ [ns]	6.25	9.17	4.35	4.98
σ_{cluster}	6.28	6.63	3.71	7.34
σ_{ray}	13.0	9.83	7.31	6.11
σ_ϕ	49.8	119	46.2	107
$\Omega(d)$ [dB]	-88.7	-108	-111	-110.7
tx_hpbw	360	60	30	15
rx_hpbw	15	15	15	15

OFDM with 128 subcarriers is considered for simulation. Simulation has been carried out for 54 wavelet namely Haar, db1 to db 10, sym 1 to sym 8, coif 1 to coif 5, bio-orthogonal family and reverse bio-orthogonal family.

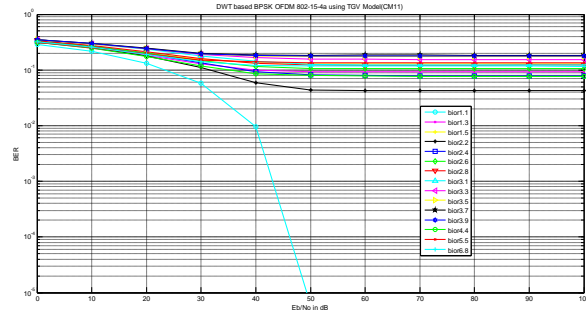
Param.	M1.5	CM2.1	CM2.2	CM2.3	CM2.4
Λ [1/ns]	0.21	0.191	0.194	0.144	0.045
λ [1/ns]	0.77	1.22	0.90	1.17	0.93
Γ [ns]	4.19	4.46	8.98	21.5	12.6
γ [ns]	1.07	6.25	9.17	4.35	4.98
σ_{cluster}	1.54	6.28	6.63	3.71	7.34
σ_{ray}	1.26	13.0	9.83	7.31	6.11
σ_ϕ	8.32	49.8	119	46.2	107
$\Omega(d)$ [dB]	--	-88.7	-108	-111	-110.7
tx_hpbw	360	360	60	30	15
rx_hpbw	15	15	15	15	15

Param.	CM3.1	CM3.2	CM4.1	CM4.2
Λ [1/ns]	0.041	0.027	0.032	0.028
λ [1/ns]	0.971	0.293	3.45	0.76
Γ [ns]	49.8	38.8	109.2	134
γ [ns]	45.2	64.9	67.9	59.0
$\sigma_{cluster}$	6.60	8.04	3.24	4.37
σ_{ray}	11.3	7.95	5.54	6.66
σ_{ϕ}	102	66.4	60.2	22.2
$\Omega(d)$ [dB]	-3.27*d -85.8	-0.303*d -90.3	-109	-107.2
tx_hpbw	30	60	360	30
rx_hpbw	30	60	15	15

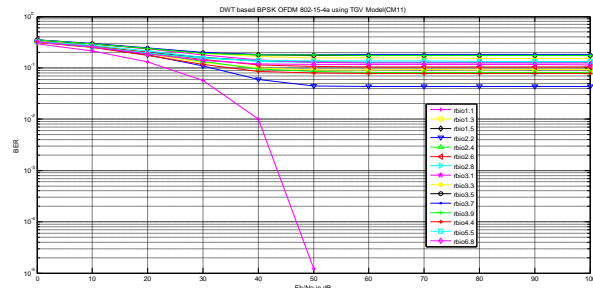
Param.	CM7.1	CM7.2	CM8.1	CM8.2
Λ [1/ns]	0.037	0.047	0.037	0.047
λ [1/ns]	0.641	0.373	0.641	0.373
Γ [ns]	21.1	22.3	21.1	22.3
γ [ns]	8.85	17.2	8.85	17.2
$\sigma_{cluster}$	3.01	7.27	3.01	7.27
σ_{ray}	7.69	4.42	7.69	4.42
σ_{ϕ}	34.6	38.1	34.6	38.1
$\Omega(d)$ [dB]	4.44*d -105.4	3.46*d -98.4	4.44*d -105.4	3.46*d -98.4
tx_hpbw	30	60	30	60
rx_hpbw	30	60	30	60



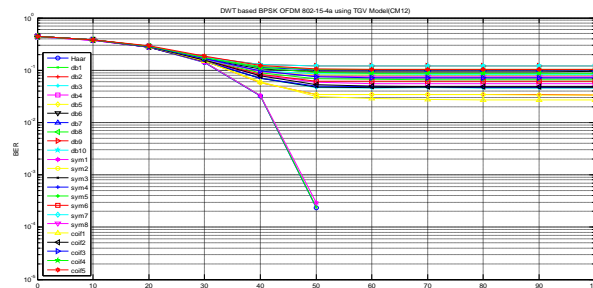
Fig(a.1):DWT-OFDM(128) for TSV model 60 GHz Channel CM11



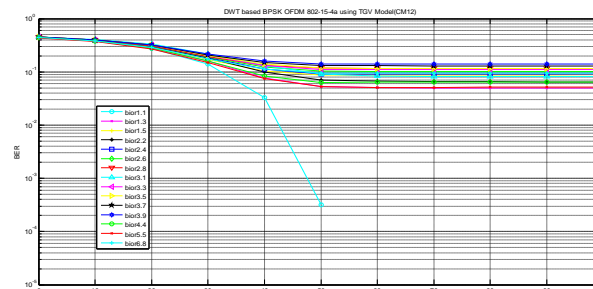
Fig(a.2):DWT-OFDM(128) for TSV model 60 GHz Channel CM11



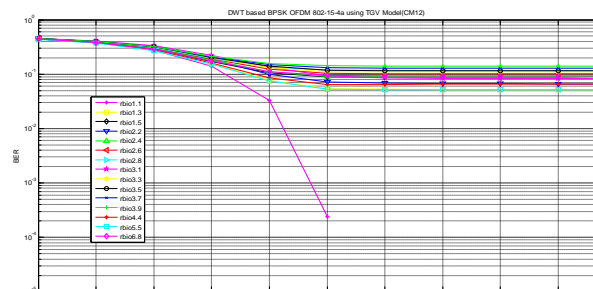
Fig(a.3):DWT-OFDM(128) for TSV model 60 GHz Channel CM11



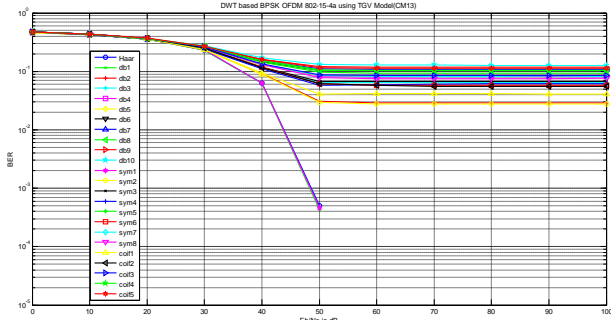
Fig(b.1):DWT-OFDM(128) for TSV model 60 GHz Channel CM12



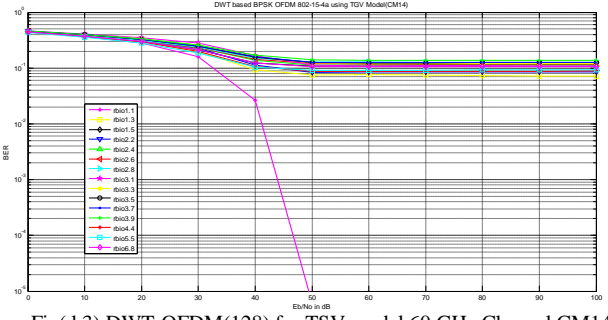
Fig(b.2):DWT-OFDM(128) for TSV model 60 GHz Channel CM12



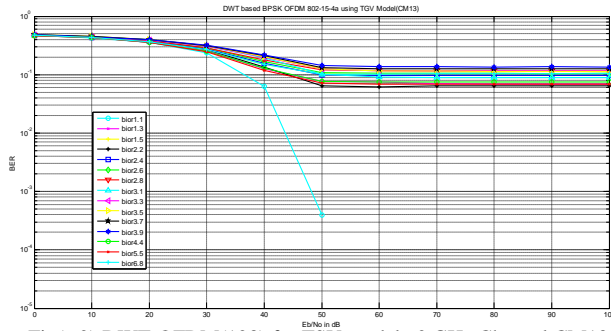
Fig(b.3):DWT-OFDM(128) for TSV model 60 GHz Channel CM12



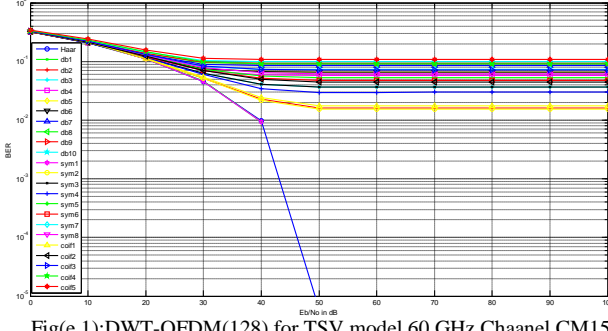
Fig(c.1):DWT-OFDM(128) for TSV model 60 GHz Channel CM13



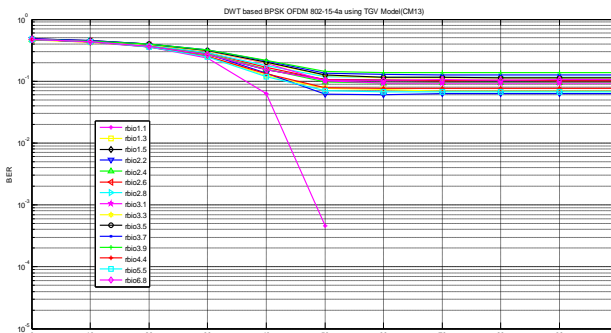
Fig(d.3):DWT-OFDM(128) for TSV model 60 GHz Channel CM14



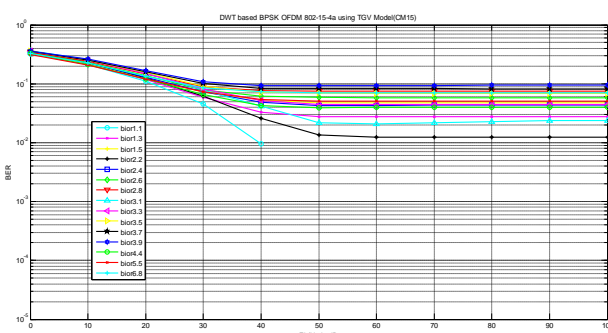
Fig(c.2):DWT-OFDM(128) for TSV model 60 GHz Channel CM13



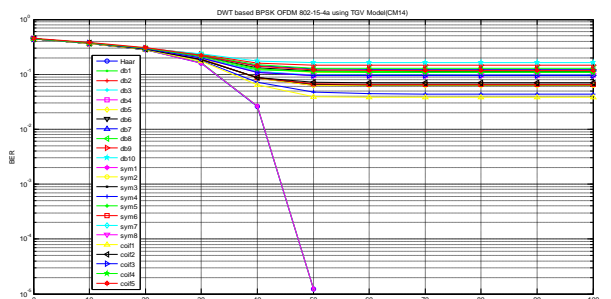
Fig(e.1):DWT-OFDM(128) for TSV model 60 GHz Channel CM15



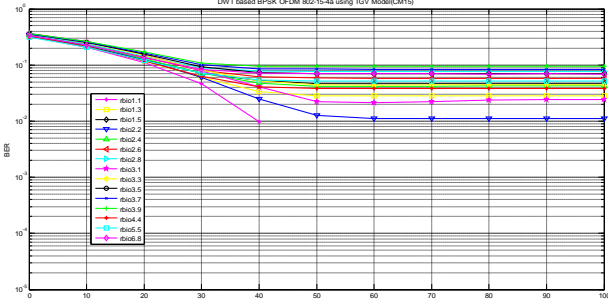
Fig(c.3):DWT-OFDM(128) for TSV model 60 GHz Channel CM13



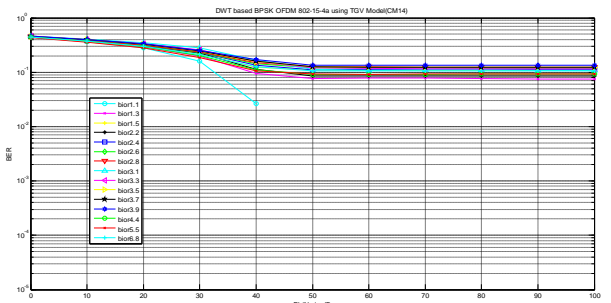
Fig(e.2):DWT-OFDM(128) for TSV model 60 GHz Channel CM15



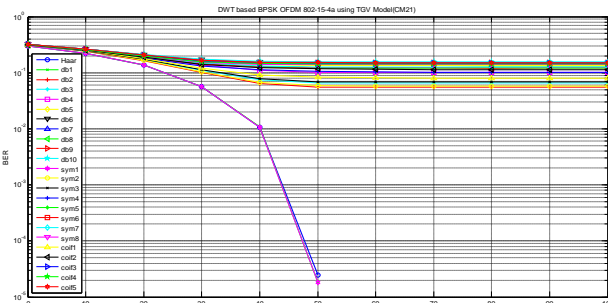
Fig(d.1):DWT-OFDM(128) for TSV model 60 GHz Channel CM14



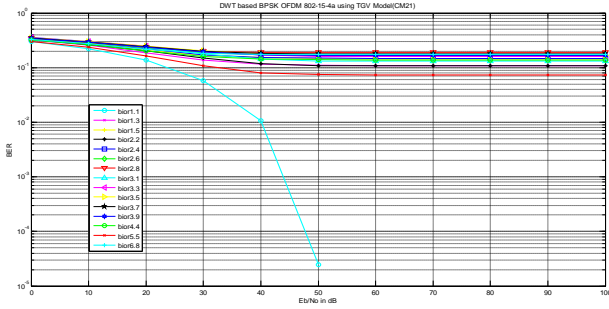
Fig(e.3):DWT-OFDM(128) for TSV model 60 GHz Channel CM15



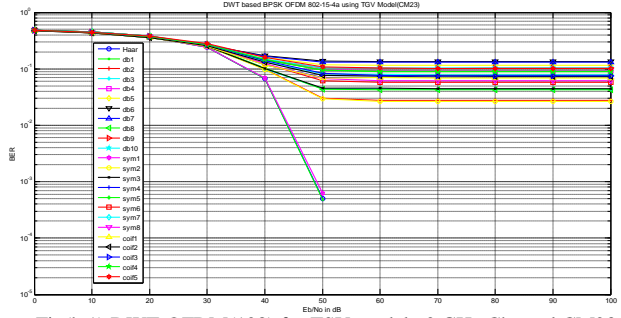
Fig(d.2):DWT-OFDM(128) for TSV model 60 GHz Channel CM14



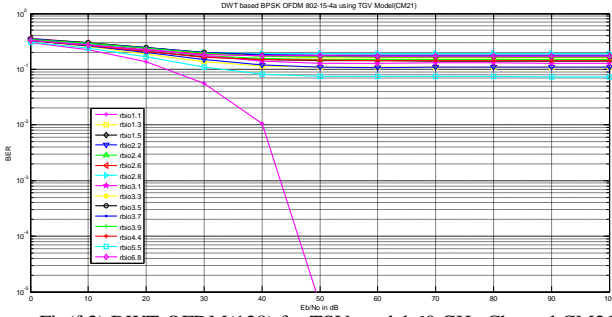
Fig(f.1):DWT-OFDM(128) for TSV model 60 GHz Channel CM21



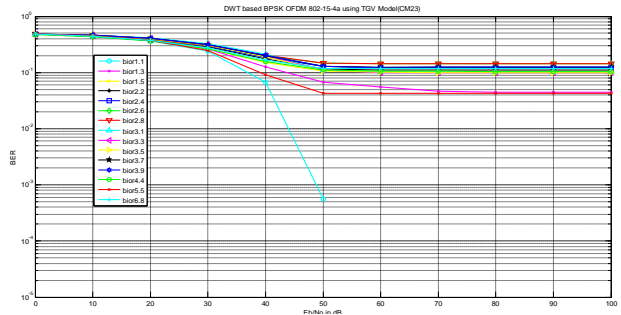
Fig(f.2):DWT-OFDM(128) for TSV model 60 GHz Channel CM21



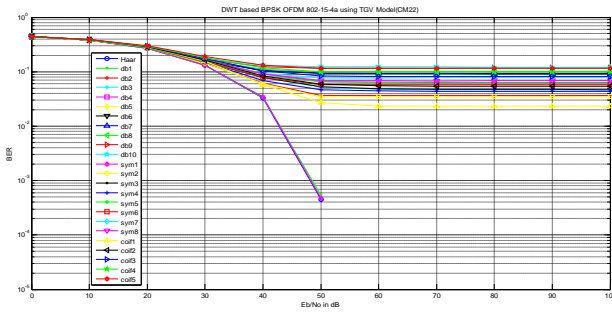
Fig(h.1):DWT-OFDM(128) for TSV model 60 GHz Channel CM23



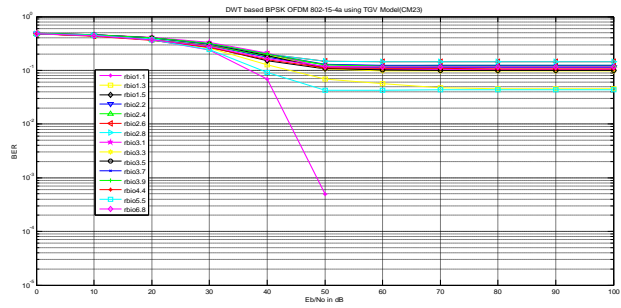
Fig(f.3):DWT-OFDM(128) for TSV model 60 GHz Channel CM21



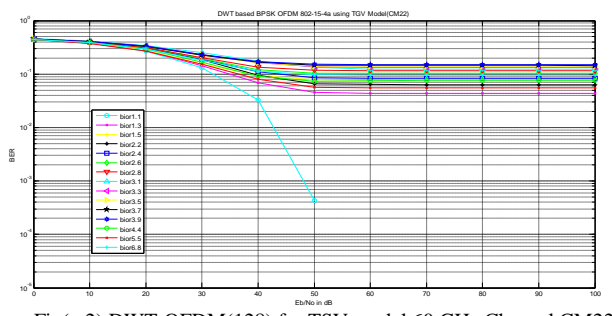
Fig(h.2):DWT-OFDM(128) for TSV model 60 GHz Channel CM23



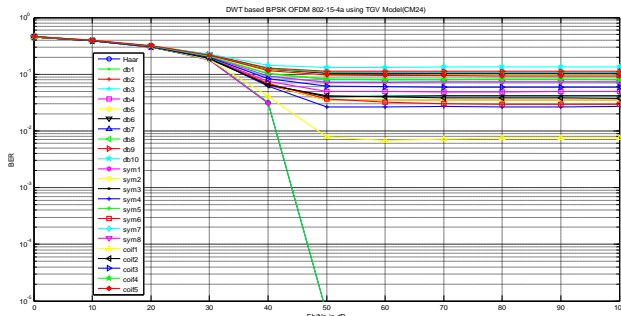
Fig(g.1):DWT-OFDM(128) for TSV model 60 GHz Channel CM22



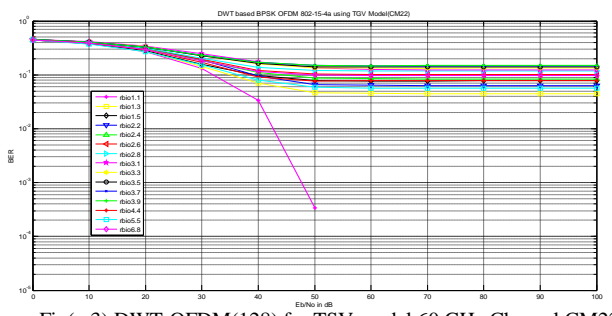
Fig(h.3):DWT-OFDM(128) for TSV model 60 GHz Channel CM23



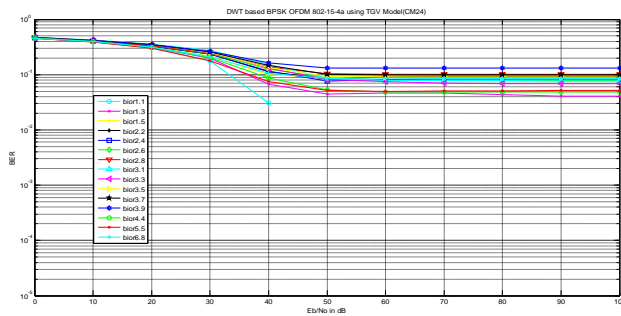
Fig(g.2):DWT-OFDM(128) for TSV model 60 GHz Channel CM22



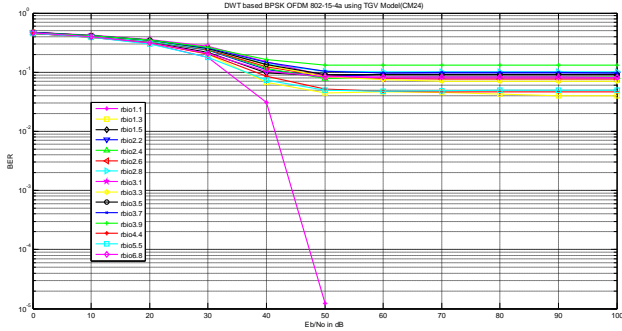
Fig(i.1):DWT-OFDM(128) for TSV model 60 GHz Channel CM24



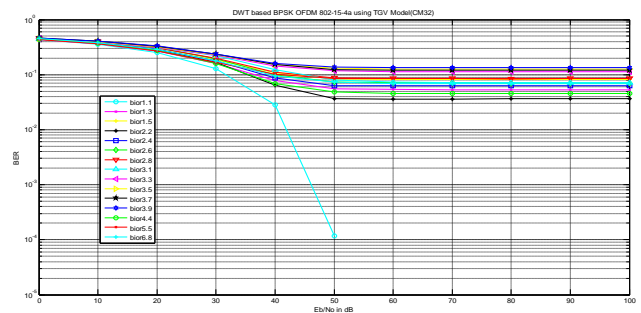
Fig(g.3):DWT-OFDM(128) for TSV model 60 GHz Channel CM22



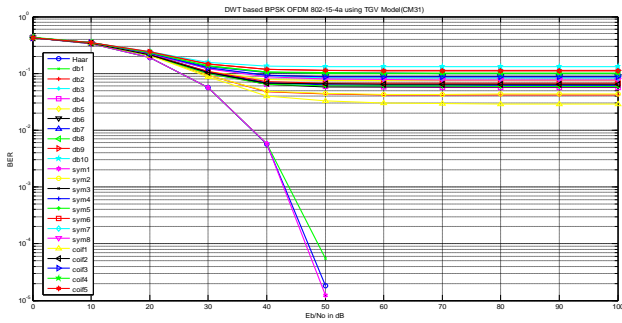
Fig(i.2):DWT-OFDM(128) for TSV model 60 GHz Channel CM24



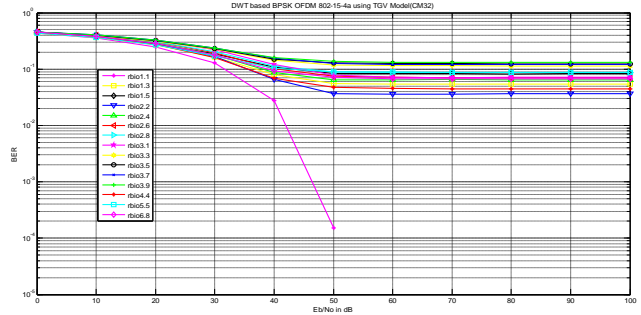
Fig(i.3):DWT-OFDM(128) for TSV model 60 GHz Channel CM24



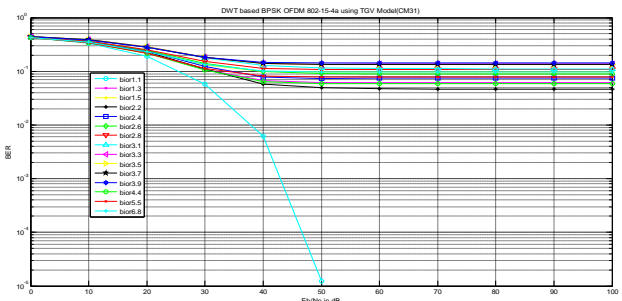
Fig(k.2):DWT-OFDM(128) for TSV model 60 GHz Channel CM32



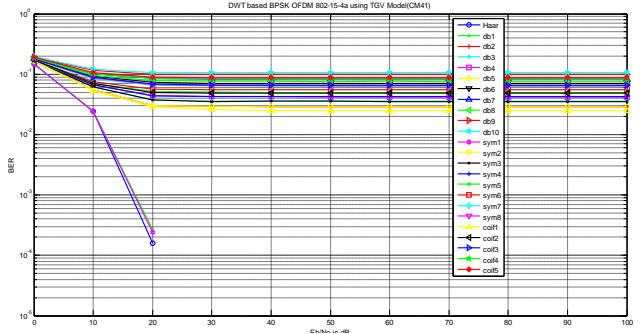
Fig(j.1):DWT-OFDM(128) for TSV model 60 GHz Channel CM31



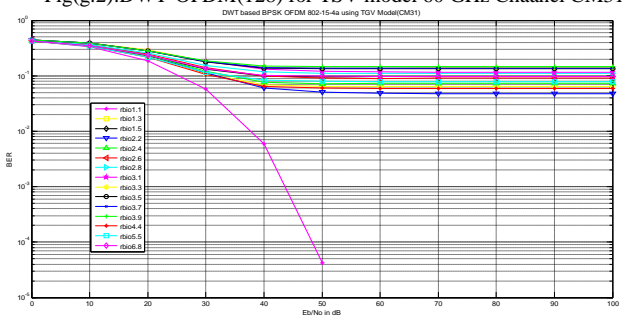
Fig(k.3):DWT-OFDM(128) for TSV model 60 GHz Channel CM32



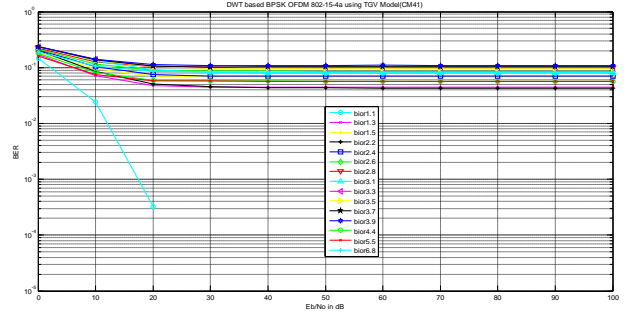
Fig(g.2):DWT-OFDM(128) for TSV model 60 GHz Channel CM31



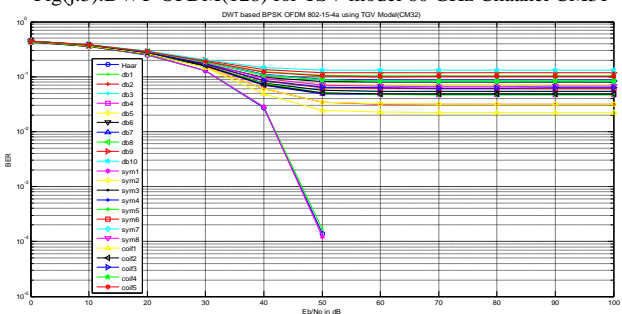
Fig(l.1):DWT-OFDM(128) for TSV model 60 GHz Channel CM41



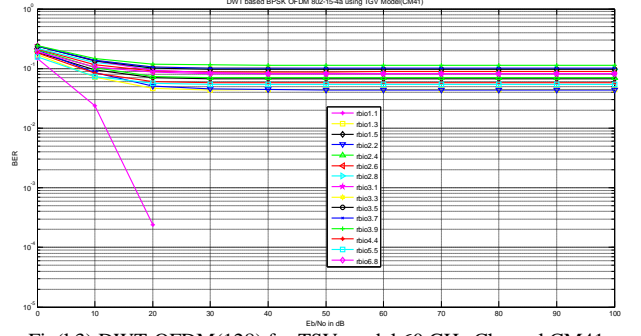
Fig(j.3):DWT-OFDM(128) for TSV model 60 GHz Channel CM31



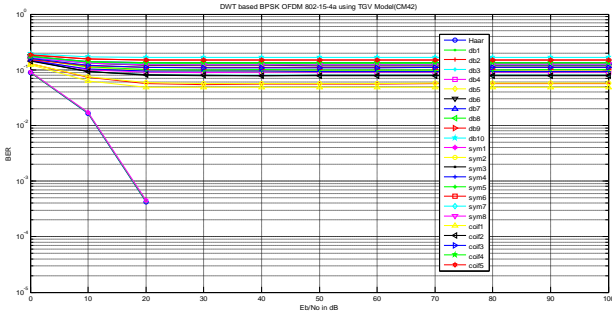
Fig(l.2):DWT-OFDM(128) for TSV model 60 GHz Channel CM41



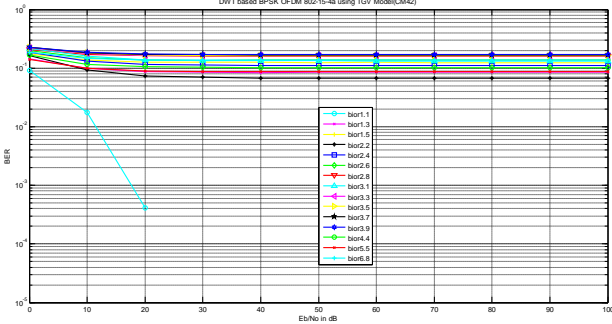
Fig(k.1):DWT-OFDM(128) for TSV model 60 GHz Channel CM32



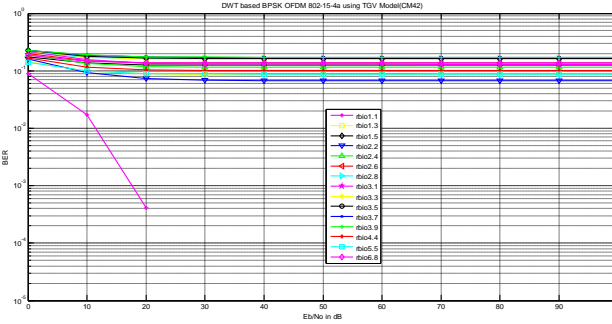
Fig(l.3):DWT-OFDM(128) for TSV model 60 GHz Channel CM41



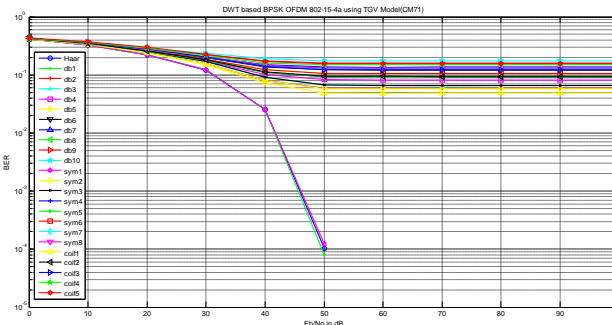
Fig(m.1):DWT-OFDM(128) for TSV model 60 GHz Channel CM42



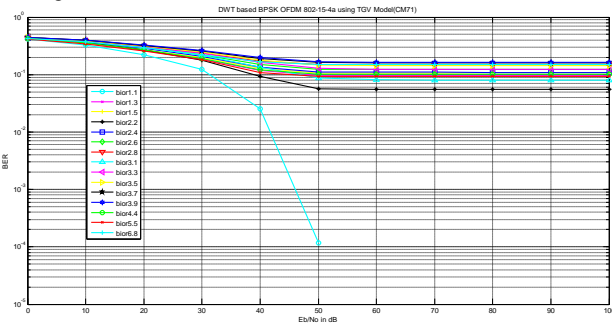
Fig(m.2):DWT-OFDM(128) for TSV model 60 GHz Channel CM42



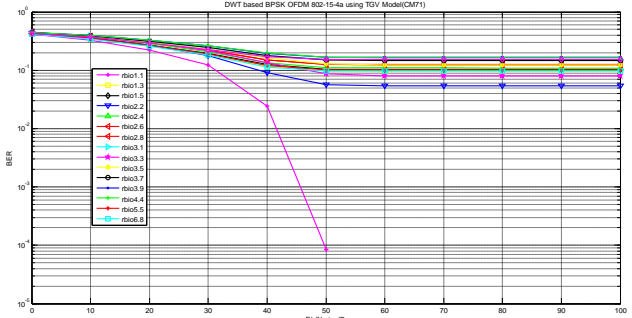
Fig(m.3):DWT-OFDM(128) for TSV model 60 GHz Channel CM42



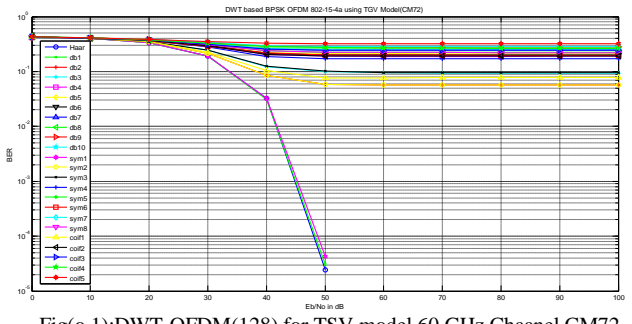
Fig(n.1):DWT-OFDM(128) for TSV model 60 GHz Channel CM71



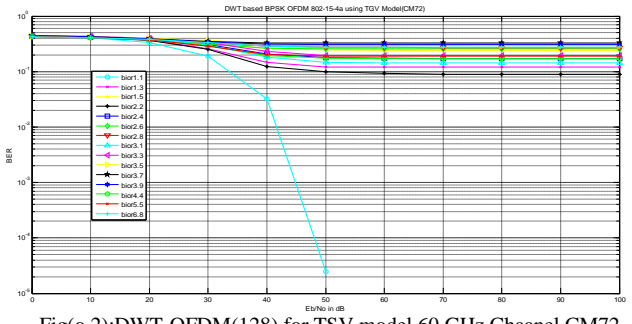
Fig(n.2):DWT-OFDM(128) for TSV model 60 GHz Channel CM71



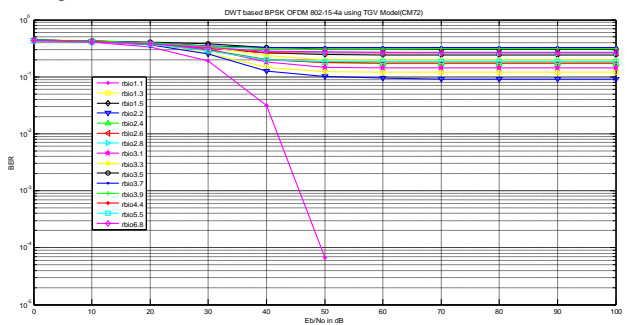
Fig(n.3):DWT-OFDM(128) for TSV model 60 GHz Channel CM71



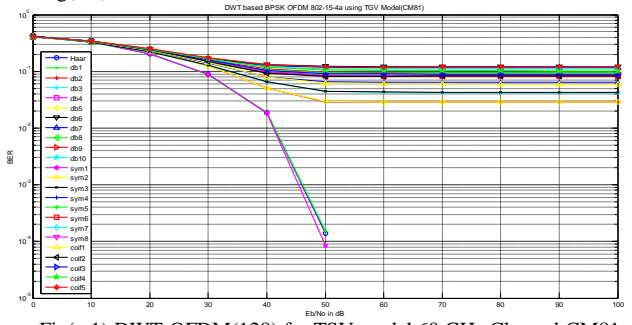
Fig(o.1):DWT-OFDM(128) for TSV model 60 GHz Channel CM72



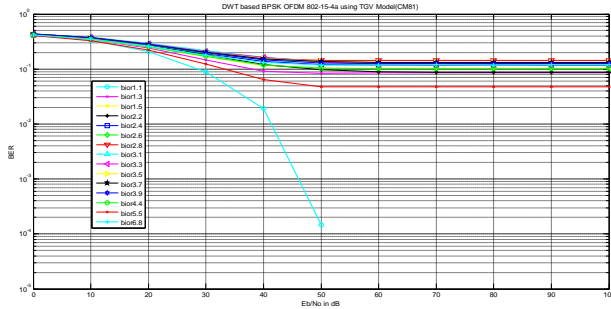
Fig(o.2):DWT-OFDM(128) for TSV model 60 GHz Channel CM72



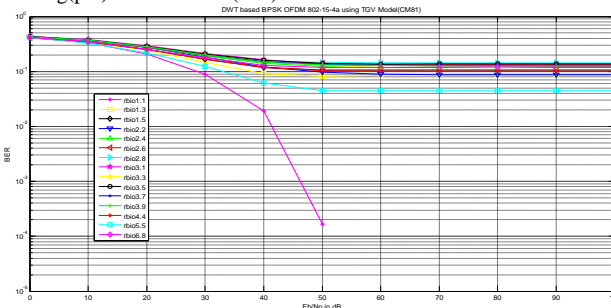
Fig(o.3):DWT-OFDM(128) for TSV model 60 GHz Channel CM72



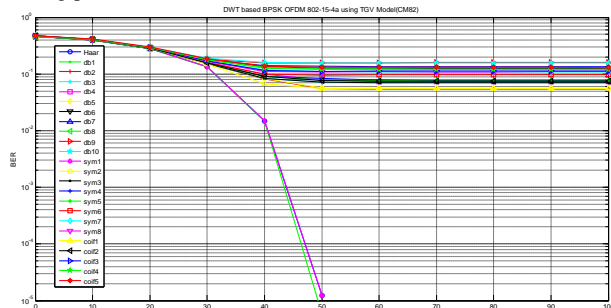
Fig(p.1):DWT-OFDM(128) for TSV model 60 GHz Channel CM81



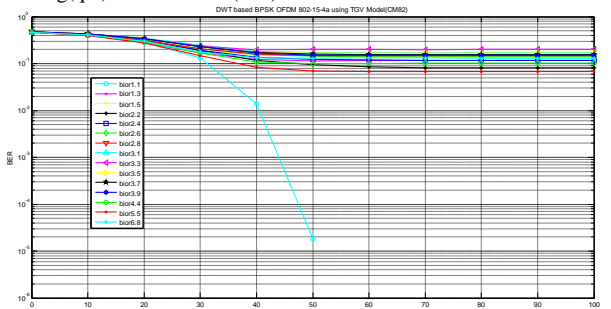
Fig(p.2):DWT-OFDM(128) for TSV model 60 GHz Channel CM81



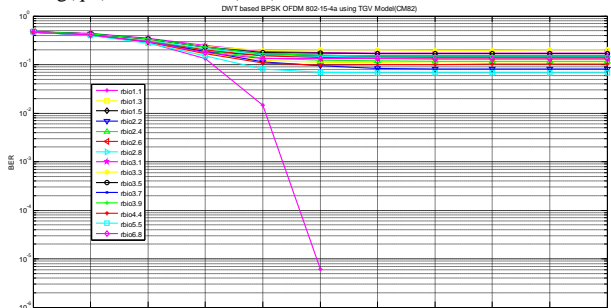
Fig(p.3):DWT-OFDM(128) for TSV model 60 GHz Channel CM81



Fig(q.1):DWT-OFDM(128) for TSV model 60 GHz Channel CM82



Fig(q.2):DWT-OFDM(128) for TSV model 60 GHz Channel CM82



Fig(q.3):DWT-OFDM(128) for TSV model 60 GHz Channel CM82

The Simulation results signify that lower order wavelets like Haar, db1, sym1, bior 1.1 and rbior 1.1 demonstrate excellent performances for all channel models. The channel model CM11 and CM14 has a better performance

as compared to CM12 and CM13 for same SNR value. Similarly channel CM21 and CM24 exhibits better performance as compared to CM22 and CM23. CM41 and CM42 exhibit very good BER performance even at a low SNR value of 20 dB. CM72 provides better BER performance over that of CM71. CM81 and CM82 have more or less similar performance; however Haar, db2 and sym1 wavelets depict excellent performance in case of CM82. As seen from figure c.1, c.2, c.3, h.1, h.2 and h.3 it observed that the performance is comparatively degraded when the transmitter half power beam width (tx_hpbw) is 30° . The results indicate good BER performance for Eb/No (SNR) above 45 dB for most of the channel models. Thus DWT OFDM demonstrates appreciable performance owing to time and frequency diversity advantage offered by wavelets. As seen from the results DWT OFDM offers distinct advantage even for complex channels at 60GHz.

V. CONCLUSION

Future generation wireless communication OFDM system is presented for DWT. The OFDM system was investigated for different types of discrete wavelet transform and various TSV model based channel at 60 GHz. As OFDM converts frequency selective channel into flat fading channel, it is very robust in frequency selective transmission. The DWT OFDM diversity scheme shows remarkable performance and robust ability in resisting impulse and narrow band noise. Thus DWT can be a good candidate for seamless broadband network in future wireless communication system.

REFERENCES

1. B. G. Negash and H. Nikookar. "Wavelet-Based Multicarrier Transmission Over Multipath Wireless Channels", IEE Electronics Letters, vol. 36, (2000) October, pp. 1787-1788.
2. A. R. Lindsey, "Generalized Orthogonally Multiplexed Communication via Wavelet Packet Bases", Ph.D. Thesis, Ohio University, (1995).
3. A. Batra, J. Balakrishnan, G. R. Aiello, J. R. Foerster and A. Dabak, "Design of a multiband OFDM system for realistic UWB channel environments", IEEE Transactions on Microwave Theory and Techniques, vol. 52, no. 9, (2004) September, pp. 2123-2139.
4. Md. Mahmudul Hasan. "Performance Comparison of Wavelet and FFT Based Multiuser MIMO OFDM over Wireless Rayleigh Fading Channel", International Journal of Energy, Information and Communications Vol. 3, Issue 4, November, 2012.
5. Mrs. Veena M.B & Dr. M.N. Shanmukha Swamy. "Performance analysis of DWT based OFDM over FFT based OFDM and implementing on FPGA", International Journal of VLSI design & Communication Systems (VLSICS) Vol.2, No.3, September 2011.
6. B. Negash and H. Nikookar, "Wavelet based OFDM for wireless channels," in IEEE VTS 53rd Vehicular Technology Conference, 2001. VTC 2001 Spring. 2001, pp. 688-691.
7. Kelvin O. O. Anoh, Raed A. A. Abd-Alhameed, Michael Chukwu, Mohammed Buhari and Steve M. R. Jones. "Towards a Seamless Future Generation Network for High Speed Wireless Communications", (IJACSA) International Journal of Advanced Computer Science and Applications, Vol. 4, No. 9, 2013.
8. Yong Soo Cho, Jaekwon Kim, Won Young Yang and Chung G. Kang, MIMO - OFDM wireless communication with MATLAB, John Wiley and Sons (Asia) Pvt. Ltd., 2010.

9. O. O. Anoh, N. T. Ali, R. Abd-Alhameed, S. M. Jones, and Y. A. Dama, "On the performance of DWT and WPT modulation for multicarrier systems," in 2012 IEEE 17th International Workshop on Computer Aided Modeling and Design of Communication Links and Networks (CAMAD), 2012, pp. 348-352.
10. A. Jamin and P. Mähönen, "Wavelet packet modulation for wireless communications," *Wireless Communications and Mobile Computing*, vol. 5, pp. 123-137, 2005.
11. [18] H. M. Ozaktas, B. Barshan, D. Mendlovic, and L. Onural, "Convolution, filtering, and multiplexing in fractional Fourier domains and their relation to chirp and wavelet transforms," *JOSA A*, vol. 11, pp. 547-559, 1994.
12. [19] B. Negash and H. Nikookar, "Wavelet-based multicarrier transmission over multipath wireless channels," *Electronics Letters*, vol. 36, pp. 1787-1788, 2000.
13. [20] B. Negash and H. Nikookar, "Wavelet based OFDM for wireless channels," in *IEEE VTS 53rd Vehicular Technology Conference*, 2001. VTC 2001 Spring, 2001, pp. 688-691.
14. [21] Y. Zhang and S. Cheng, "A novel multicarrier signal transmission system over multipath channel of low-voltage power line," *IEEE Transactions on Power Delivery*, vol. 19, pp. 1668-1672, 2004.
15. K. Abdullah and Z. M. Hussain, *Studies on DWT-OFDM and FFT-OFDM Systems*, *IEEE International Conference on Communication, Computer and Power*, February 15-18, 2009.
16. W. Saad, N. El-Fishawy, S. EL-Rabaie, and M. Shokair, *An Efficient Technique for OFDM System Using Discrete Wavelet Transform*, Springer-Verlag Berlin Heidelberg, pp. 533-541, 2010.
17. H. Harada, R. Punada, H. Sawada, C H Choi and Y Shoji, "IEEE 802.15.4a channel model", 2006.